



# THE APPLICATION OF A LINEAR MICROPHONE ARRAY IN THE QUANTITATIVE EVALUATION OF THE BLADE TRAILING-EDGE NOISE REDUCTION

Luqin Mao, Xiang Kangshen, Fan Tong, Liang Ji, and Weiyang Qiao<sup>§</sup>  
School of Power and Energy, Northwestern Polytechnical University  
West Youyi Road 127#, 710072, Xi'an, China

## ABSTRACT

This study concerns the application of a linear microphone array in the quantitative evaluation of the blade trailing-edge noise reduction with serrated trailing edge configuration in an indoor open jet wind tunnel test bed based on Clean-SC algorithm. In order to obtain correct application and to achieve the best effect for the microphone array test, the computing software for microphone array data processing based on Clean-SC algorithm is firstly developed and is assessed by Sarradj's benchmark synthesized input data. The assessment results show that the present array data processing software based on Clean-SC algorithm has a good accuracy with an error of less than 0.5 dB in a wide frequency range. Then, a linear array of 32 microphones was used to identify the trailing-edge noise of NACA65 (12)-10 blade with a chord length of 150 mm and with a span of 300mm. The comparison and analysis of the Clean-PSF and Clean-SC algorithms for the experimental identification the leading-edge and trailing-edge noise sources of the blade are investigated. The results show that there is about 2dB error in noise source identification by using Clean-PSF algorithm because of the interference between the different aerodynamic noise sources. At last, experimental studies are performed to investigate the trailing-edge noise reduction of the NACA65 (12)-10 blade using serrated trailing edge configuration. The trailing-edge noise for the blade with and without sawtooth configuration were measured with the flow speeds of  $U=20\text{m/s}$  to  $70\text{m/s}$ , and the corresponding Reynolds numbers based on the blade chord are in  $200,000 \sim 700,000$ . Parametric studies of the sawtooth amplitude and wavelength are conducted in order to understand the effect of sawtooth configuration on trailing-edge noise reduction. It is found that the TE noise reduction is sensitive to both the amplitude and wavelength of the serrated trailing edge configuration. The flow speed and the angle of attack will also affect the noise reduction of serrated trailing-edge. In order to obtain the best noise reduction effect, the sawtooth configuration should be carefully designed according to the actual working conditions and air flow parameters.

---

<sup>§</sup> Correspondence author: Professor, Northwestern Polytechnical University, Qiaowu@nwpu.edu.cn

## 1 INTRODUCTION

The reduction of the turbulence broadband noise from the trailing-edge (TE) and leading-edge (LE) of airfoil or the turbomachinery blade is nowadays an important industrial need and probably one of the most challenging issues in aero-acoustics[1]. TE noise which results from the interaction between the turbulent boundary layers (TBL) that grow on the airfoil/blade and the sharp trailing edge. As a typical aerodynamic noise source, trailing-edge noise has been widely studied. Especially, being cognizant of an overestimate in the case of the infinite plane and an underestimate in the case of the hard semi-infinite plane for the edge noise with the simple application of Curle's theory[2], considerable progress has been made towards a clarification of various surface effects. The first essential results and theoretical understanding of the trailing-edge problem is due to Ffowcs Williams and Hall[3]. Based on the solution of Lighthill' acoustic analogy equation with an appropriate Green's function, they showed that the far-field intensity of the sound field produced by turbulence past trailing edge varies with  $U^5$  and scales with a typical flow velocity  $U$  as  $U^5$ . After Ffowcs Williams and Hall, many researchers worked on edge noise to understand and predict of this noise, such as Crighton & Leppington[4], Crighton[5], Chandiramani[6], Levine[7], Howe[8,9], Chase[10,11], Davis [12], and Howe[13]. Based on the above theoretical studies, the TE noise has been characterized experimentally by Brooks et al.[14,15] and successfully modeled by Amiet[16,17] and Howe[18].

The reduction of TBL-TE noise has been a matter of concern since 1930s[19], and the ability to fly silently of most owl species has long been a source of inspiration for finding solutions for quieter aircraft and turbomachinery [20,21]. Inspired by the quiet flying Owl, the noise reduction effect of porous treatment are investigated by Bohn, Khorrami and Sarradj al. [22-24] Brushes have also proved to be efficient noise reduction devices in the studies of Finez & al.[25]. The present study deals with another noise reduction concept which is firstly proposed by Howe[26,27]. It is argued that the gusts with wavenumbers normal to the TE have higher radiation efficiency than oblique gusts; and that, there are more normal wavenumbers for the straight trailing edge because the main flow direction is often almost normal to the TE. Consequently an "oblique TE" should reduce the sound generation and the noise levels accordingly. Howe studied analytically a sinusoidal TE[26] and a sawtooth TE[27]. Both geometries are defined by the wavelength of serrations  $\lambda$  and their amplitude  $h$ . Assuming the Mach number is vanishing and that the turbulent eddies are not affected by the serrations in the vicinity of the TE, Howe predicted a noise reduction of  $10 \times \log_{10}(Ch/\lambda)$  (dB) where  $C \approx 10$  for  $\lambda/h \leq 4$  for the sinusoidal TE and of  $10 \times \log_{10}(1+(4h/\lambda)^2)$  (dB) when  $\omega h/U \approx 1$  for the sawtooth TE. Following Howe's encouraging theoretical work, many experimental studies assessed the acoustic benefit of serrated TE, and serrations reveal to be a robust noise reduction device since the reduction occurs for all airfoils [28,29].

However, the present aero-acoustic theory of TE noise and LE noise does not meet the needs of the reduction of the turbulence broadband noise of airfoil or the turbomachinery blade. For example, it is found that Howe's theoretical model over-predicted very large noise reduction levels with serrated trailing-edge in some frequency, and lowly-predicted very much the noise suppression with serrated trailing-edge in other frequency range [30]. It is proposed that the flow and acoustic mechanism of the real airplane wing and turbomachinery blade are more sophisticated than that of semi-infinite plane due to the elaborate loading distribution, flow turn, the change of flow attack angle in the real blade. Especially, there is a complicated interrelationship between leading-edge flow and trailing-edge flow for the real

blade due to the small chord [30]. The LE noise source and TE noise source always arise simultaneously, and these two sources are always very closer each other in real blade. In order to understand the mechanism of LE and TE noise, and to evaluate the noise reduction of the airfoil and blade turbulence noise, it is necessary to separate and quantify the airfoil LE and TE noise source in the experimental research. Especially, because the most aerodynamical and performance tests are mostly carried out in the indoor test bed, and not all aeroacoustic test could be done in a perfect anechoic room. There will be very strong background noise which will contaminate the LE and TE noise radiation in these tests. It would be key to separate and quantify the airfoil LE and TE noise source to get the useful aeroacoustic information.

Acoustic beamforming with microphone phased-array is a powerful method to investigate the flow noise emission. This technique has been largely used in aeronautics to investigate and characterize aerodynamic noise, and has become a standard method for localizing the noise sources on aircraft, trains, cars and other machinery. The performance of conventional beamforming depends to a large extent on a good design of the array geometry and on a good beamforming software. The recent developments of inverse methods make it possible for the first time to determine the strengths of the sources[31-35]. To obtain higher resolution acoustic source plots from microphone array measurements, deconvolution techniques are becoming increasingly popular. Deconvolution algorithms aim at identifying Point Spread Functions (PSF) in source plots, and may therefore fall short when actual beam patterns of measured noise sources are not similar to synthetically obtained PSF's. To overcome this, the new version of the classical deconvolution method Clean is proposed: Clean-SC. By this new method, which is based on spatial source coherence, side lobes can be removed in measured beam patterns. Essentially, Clean-SC iteratively removes the part of the source plot which is spatially coherent with the peak source. A feature of Clean-SC is its ability to extract absolute sound power levels from the source plots[36].

This study concerns the application of a linear microphone array in the quantitative evaluation of the blade trailing-edge noise reduction with serrated trailing edge configuration in an indoor open jet wind tunnel test bed based on Clean-SC algorithm. The computing software for microphone array data processing based on Clean-SC algorithm is developed and assessed by Sarradj's benchmark synthesized input data. A linear array of 32 microphones was used to identify the leading-edge noise and trailing-edge noise of NACA65 (12)-10 blade with a chord length of 150 mm and with a span of 300mm. The trailing-edge noise for the blade with and without sawtooth configuration were measured with the flow speeds of  $U=20\text{m/s}$  to  $70\text{m/s}$ , and the corresponding Reynolds numbers based on the blade chord are in  $20,000 \sim 70,000$ . Parametric studies of the sawtooth amplitude and wavelength are conducted in order to understand the effect of sawtooth configuration on trailing-edge noise reduction.

## **2 THE ASSESSMENT OF THE ARRAY DATA COMPUTING SOFTWARE USING SARRADJ'S BENCHMARK SYNTHESIZED INPUT DATA**

The benchmark synthesized input data proposed by Sarradj et al.[37] are used to assess the present array data reduction program which is based on the Clean-SC algorithm. The benchmark synthesized input data includes four monopole sources at the corners of an 0.2 m by 0.2 m square. The sources are located at 0.75 m distance (the coordinates are respectively (0.1 m, -0.1 m, 0.75 m), (-0.1 m, -0.1 m, 0.75 m), (-0.1 m, 0.1 m, 0.75 m), (0.1 m, 0.1 m, 0.75 m)).

m)) from an array of 64 microphones. The array has a seven arms logarithmic spiral arrangement and an aperture of approximately 1.5 m, see figure 1. Two subcases are considered: subcase A: All sources have the same power. subcase B: The sources all have different power. One source has a power level that is approximately 6 dB less than the strongest source. Two more sources have a power approximately 12 dB and 18 dB less than the strongest source, respectively.

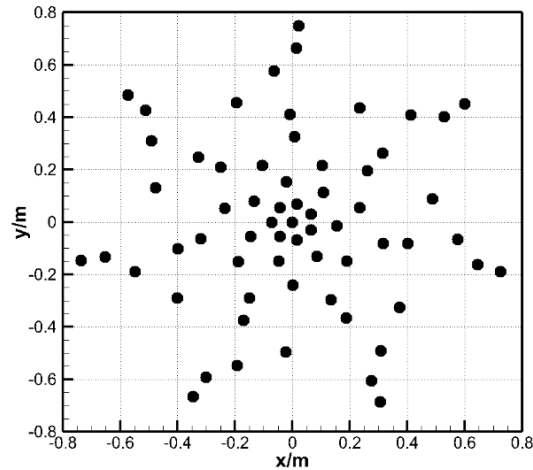
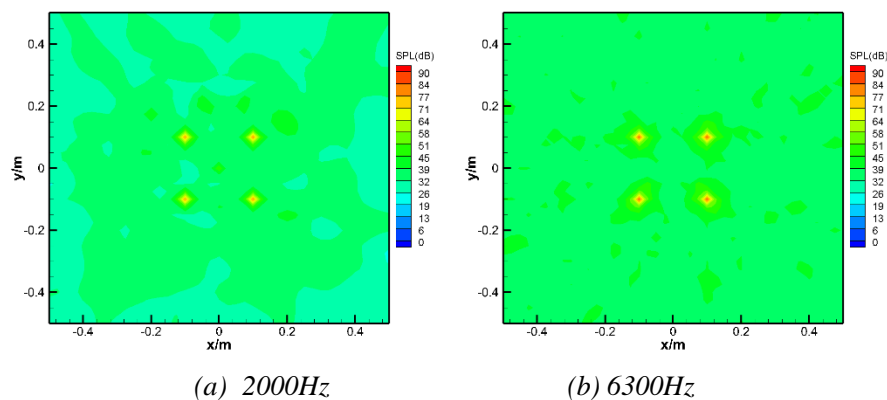


Figure 1. Arrangement of the 64 array microphones

As indicated by Sarradj et al.[37], independent random number generators with a normal distribution are used for each of the sources. Consequently, the contributions of the individual sources at each of the microphones are uncorrelated. To obtain the microphone signals, the source signals are first delayed by an appropriate amount of time and afterwards they are superposed for each individual microphone. The microphone signals are then sampled with a rate of 51.2 kHz. From the microphone signals, the CSM is computed using 999 frames of 1024 samples each with a Hanning window applied and 50% overlap. The CSM thus contains values for 513 frequencies (multiples of 50 Hz).

## 2.1 Results for Subcase A

Figure 2 is the sound source distribution on different frequencies of the subcase A obtained by the present microphone array data processing program based on Clean-SC algorithm. It can be seen from figure 2 that the program used in this paper can accurately identify the location of the noise source, and get a very clean image of the sound source.



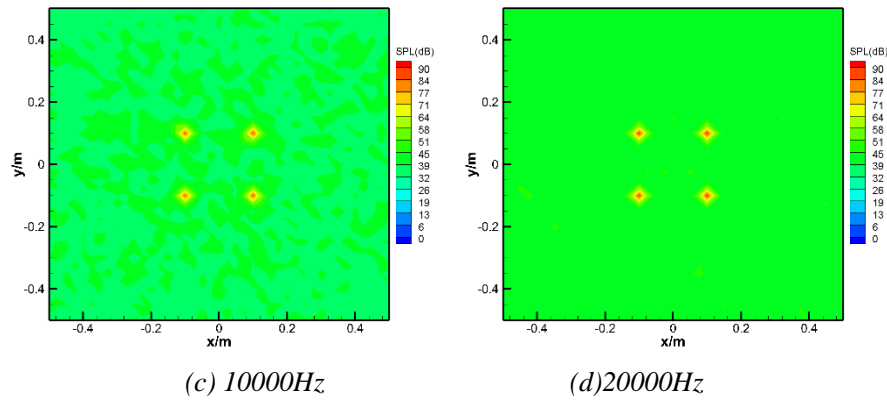


Figure 2. Sound source distribution for subcase A on different frequency

Figure 3 shows the comparison between the identification results of four sound sources and the benchmark data for subcase A. As can be seen from Figure 3, the magnitude of four sound sources are accurately identified using the present array data processing software based on Clean-SC algorithm.

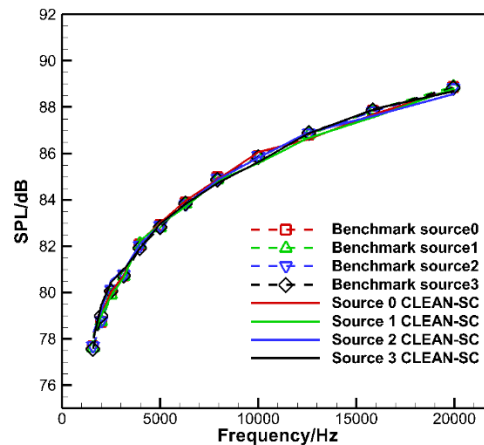
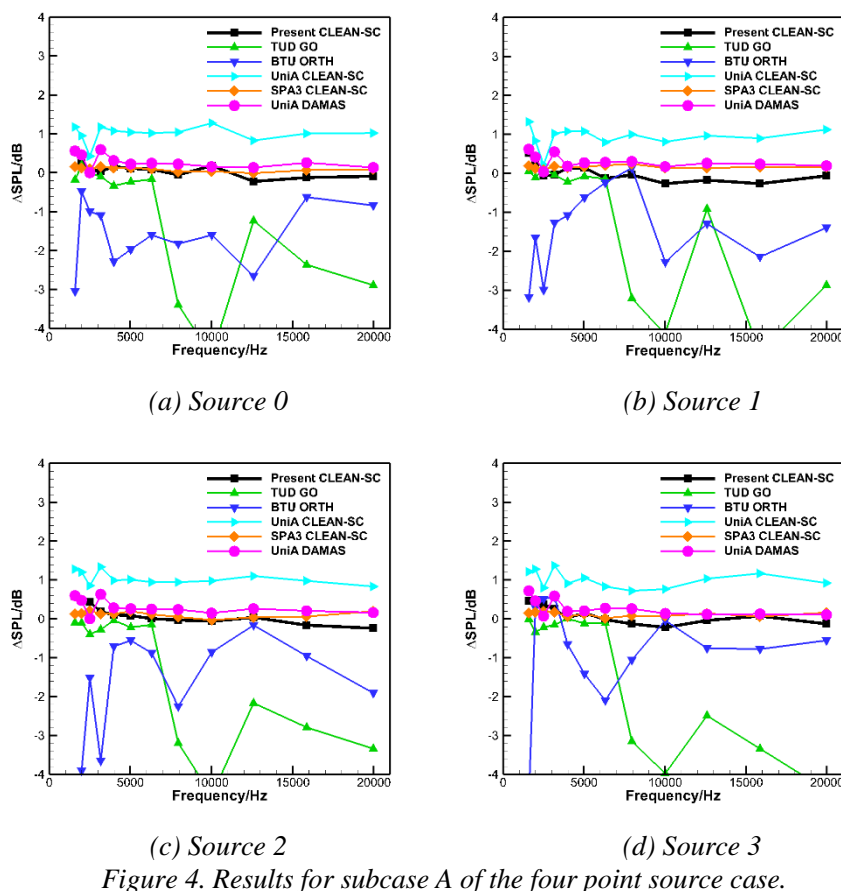


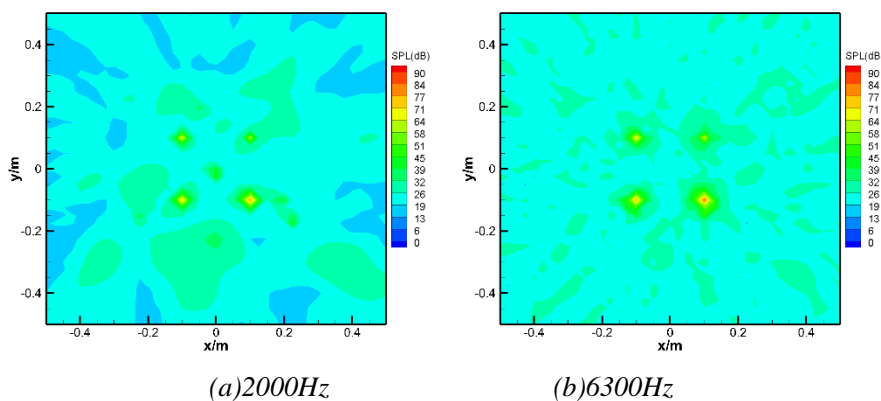
Figure 3. Results for subcase A of the four point source case

Figure 4 shows the difference between present identification results and benchmark data. For more extensive comparison, the results of other researchers are also shown in the figure, including BTU, UniA, NASA, TUD[37]. It can be seen from figure 4 that the present array data processing software based on Clean-SC algorithm has a good accuracy in a wide frequency range, with an error of less than 0.5 dB, and an error of less than 0.2 dB in a frequency range higher than 3000 Hz.



## 2.2 Results for Subcase B

Figure 5 is the sound source distribution on different frequencies of the subcase B obtained by the present microphone array data processing program based on Clean-SC algorithm. It can be seen from figure 5 that, even for the complex sound sources in subcase B, the present program can accurately identify the location of the noise source, and get a clean image of the sound source.



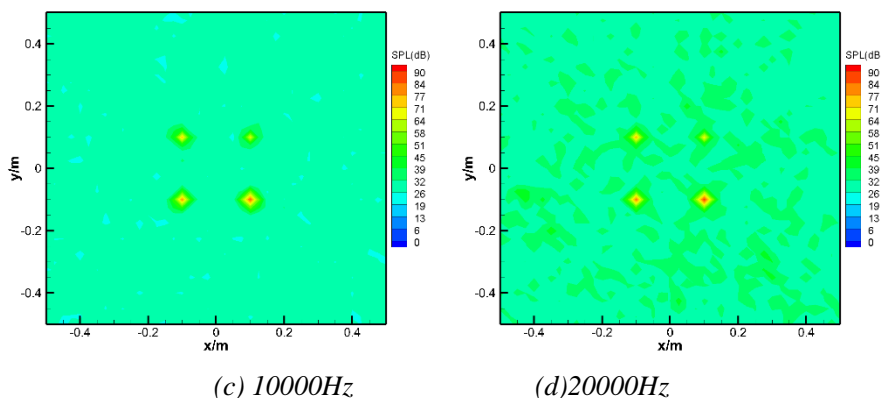


Figure 5. Sound source distribution for subcase B on different frequency

Figure 6 shows the comparison between the identification results of four sound sources and the benchmark data for subcase B. As can be seen from figure 6, although the four sources differ in intensity by up to 18 dB (which means 63 times the energy difference), the magnitude of four sound sources are accurately identified using the present array data processing software based on Clean-SC algorithm.

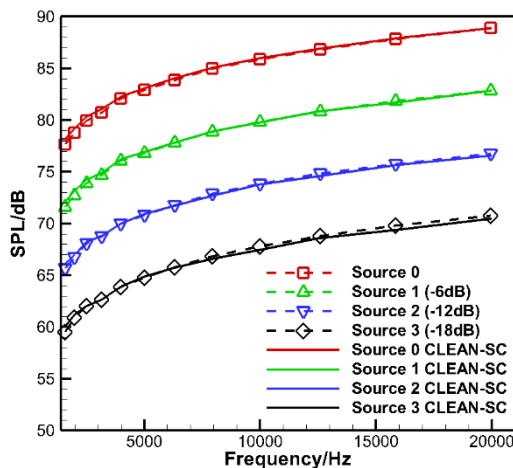


Figure 6. Results for subcase B of the four point source case

Figure 7 shows the difference between present identification results and benchmark data. For more extensive comparison, the results of other researchers are also shown in the figure. Compared with figure 4 and 7, it can be seen that accurate identification of non-equal intensity complex sound sources requires higher algorithm, especially for the accurate identification of the weakest sound source (-18 dB). It can be seen from figure 8 that for the weakest sound source 3, only the array identification methods of PSA3 and present paper based on Clean-SC algorithm can achieve high accuracy, which the error above 3000hz is less than 0.2db, and have good robustness. The error of the array identification method of UniA based on Clean-SC algorithm is within 1 dB in subcase A, however, in more complex subcase B, the calculation error increases significantly. For the weakest source 3, the error of the array identification method of UniA can reach 3 dB. This also shows that although Clean-SC

algorithm has been proposed for a long time, it still needs special attention to its correct application to achieve the best effect, which fully verifies the importance of Sarradj's works.

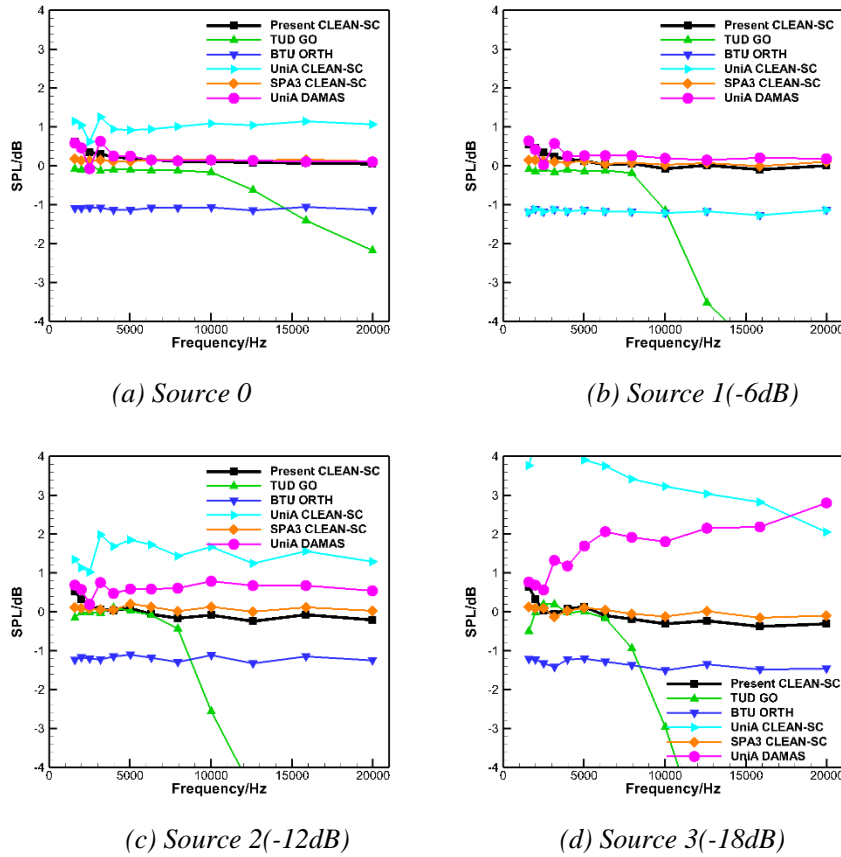


Figure 7. Results for subcase B of the four point source case.

### 3 THE APPLICATION OF A LINEAR MICROPHONE ARRAY IN THE IDENTIFICATION OF LE AND TE NOISE SOURCE

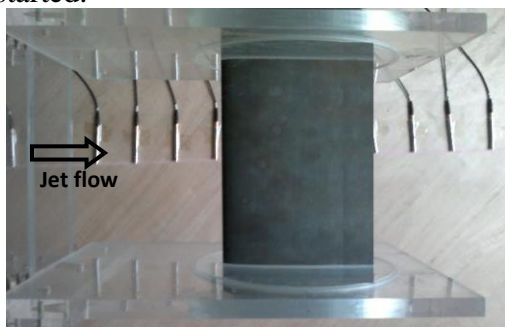
#### 3.1 Experimental set-up

The experiment was carried out in the low speed open jet wind tunnel in Northwestern Polytechnical University, and the NACA65 (12)-10 blade was tested. The wind tunnel can be broken up into two major sections: the upstream section and the test section. The upstream section consists of the centrifugal fan, the settling screens, the diffuser and the contraction. Flow is supplied to the tunnel through a centrifugal fan which is powered by a 20 Kw AC motor. After passing through the fan, the flow is slowed down through a diffuser before entering the settling chamber. The total length of the diffuser and the settling chamber is about 2 m while the expansion ratio from the exit of the fan to the settling chamber is 1:5.75. Before exiting the settling chamber and entering the contraction, the flow passes through flow conditioning screens to reduce the turbulence levels and swirling. The contraction, with a contraction ratio of 1:8.22 directs the flow into the test section. The test section is shown in figure 8, the open jet of wind tunnel exit with a 0.3 m×0.09 m rectangular channel. Air is supplied by the wind tunnel at Mach numbers ranging up to 0.3. The turbulence intensity at outlet of the wind tunnel is keep below 1%.

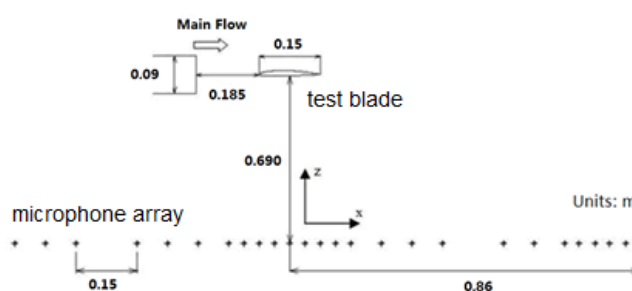
A NACA65 (12)-10 blade with a 150 mm chord and 300 mm span, is placed into the core of an open jet of the tunnel exit which is shown in Fig. 8. The blade is mounted onto a plexiglass disk, which allows tuning the angle of attack  $\alpha$  from  $-5$  to  $+5$  degree as shown in figure 8(a).

An unequal spacing linear microphone array with 32 microphones (Fig. 8(b)) was used to identify the sound source around airfoil and to analysis the noise strength and spectra. The array was placed just underneath the airfoil about 0.690 m and the centre of the array was placed underneath the centre of blade. The all microphone with its diaphragm is mounted on a large, hard reflecting surface so that the sound pressure levels obtained will be augmented over the whole spectrum, up to the frequency at which incident and reflected waves interfere, by a factor of 2 (6 dB) (as shown Fig. 8(a)). It must be noted that, in order to remove the background noises of the indoor open jet wind tunnel test, the correction methods for the effects of reverberation and shear layer on sound propagation which is developed by our group[38] was used in this test.

The  $\frac{1}{4}$  inch capacitive microphones produced by BSWA Company are used. Frequency range of this type microphone is from 20 Hz to 20 kHz in free field, and sound pressure levels up to 168 dB. The sensitivity is 5 mV/Pa. The microphone has an operating temperature range of  $-50$  to  $+110$  degree Celsius, and with a main ambient temperature coefficient of 0.01 dB/K and a main ambient pressure coefficient of  $-10$ -5 dB/Pa. The  $\frac{1}{4}$  inch measuring microphone preamplifier is a high-impedance transducer for condenser measuring microphone cartridges. It permits a wide-band measurements and sound level measurements with a dynamic range from 17 up to 168 dB. Its frequency range is from 1 Hz to 1 MHz. The microphone preamplifiers were connected to the BBM data acquisition system. The maximum sampling rate of the BBM system was 102.4 KHz. All microphone signals were simultaneously sampled with an AD conversion of 16-bit at a sampling frequency of 32768 Hz. The recording time for one measurement was 10 s. The calibration constants of microphones were obtained by using a 1000 Hz single frequency standard sound source before the measurement started.



(a) NACA65 (12)-10 blade and microphones



(b) test set-up

Figure 8. Microphone array and the test fit

### 3.2 LE and TE Noise Sources Identification

The NACA65 (12)-10 blade LE and TE noise are tested with different flow velocities and different angles of attack. The flow speeds are of  $U=20$  m/s, 40m/s, 60m/s and 70 m/s, and the corresponding Reynolds numbers based on the blade chord are respectively of 200,000 to 700,000. Figure 9(a) shows the beamforming results. It could be seen that, a very “clean” noise source identification is obtained with the present array measurement method. The wind

tunnel jet noise source(WT noise), the LE noise source and the TE noise source are all identified.

In order to further explain the correlation between blade leading edge noise and trailing edge noise, Clean-PSF algorithm was also used to identify the LE noise source and TE noise source, and the results was compared with that from the Clean-PSF algorithm. As shown in figure 9(b), the results obtained by the two algorithms are slightly different.

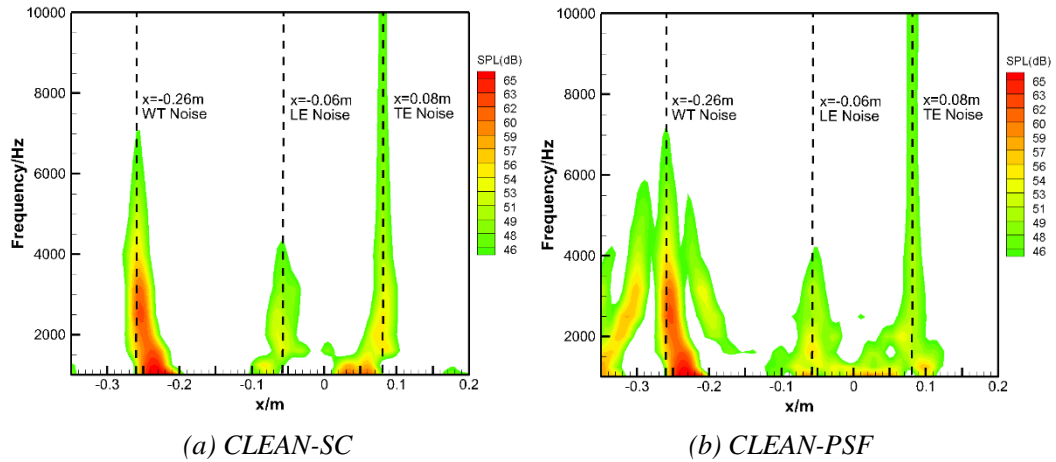
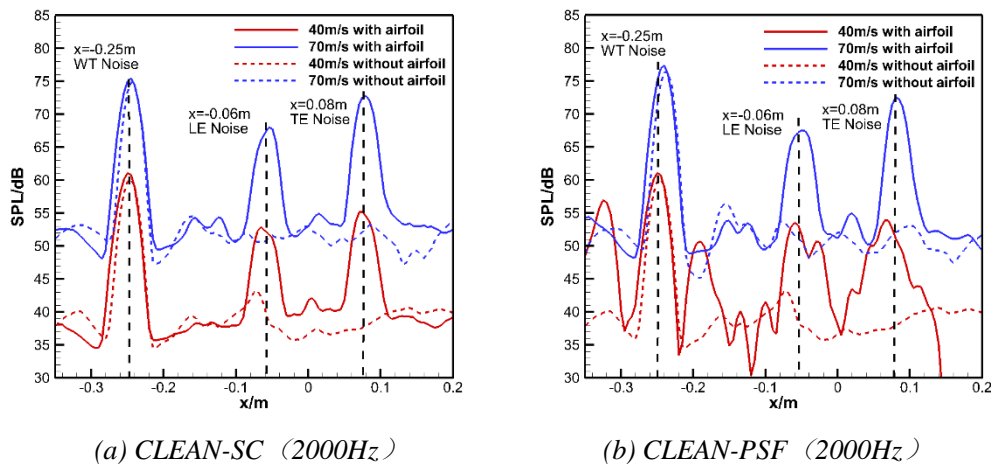


Figure 9. The beamforming results of the blade test in the open jet wind tunnel( $U = 40$  m/s)

Figure 10 is a comparison of the sound source identification results with Clean-PSF algorithm and Clean-SC algorithm. It can be found that the result with Clean-PSF algorithm has more sidelobes, while the results with Clean-SC algorithm has fewer sidelobes. There are two obvious sidelobes at  $x = -0.32$  m and  $x = -0.18$  m near the noise source of wind tunnel in the results with Clean-PSF algorithm. Further detailed comparison of figure 10 (a) and figure 10 (b) shows that the noise level of the sound source identified by PSF algorithm is about 2dB higher than that identified by SC algorithm.



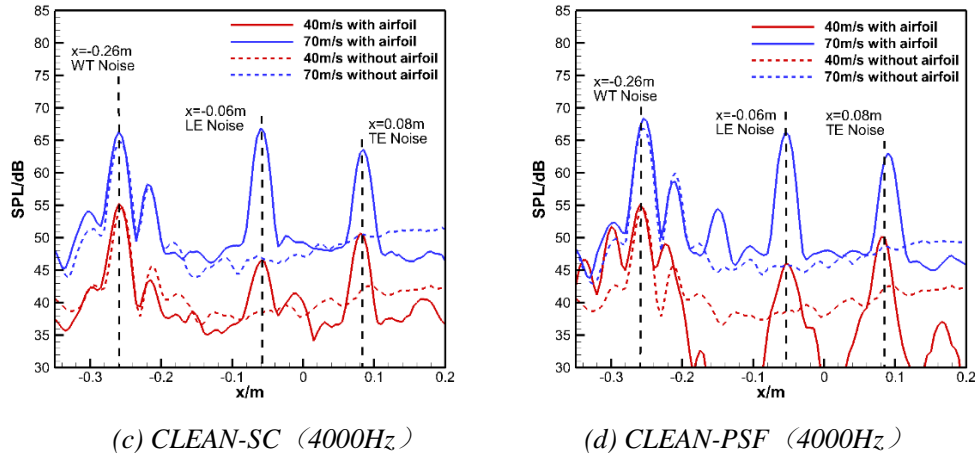
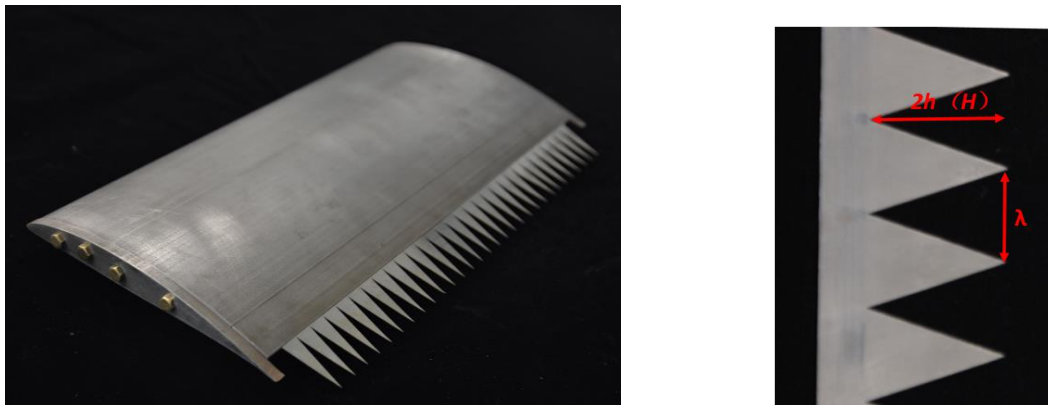


Figure 10. The comparison of the sound source identification results with Clean-PSF algorithm and Clean-SC algorithm

## 4 INVESTIGATION OF THE TRAILING-EDGE NOISE REDUCTION WITH SERRATED CONFIGURATION USING LINEAR MICROPHONE ARRAY

### 4.1 Serrated Trailing-edge Configurations

The trailing-edge noise reduction with serrated configurations for NACA65 (12)-10 blade was experimentally investigated using the same linear array. In order to systematically parameterize the noise reduction effect and regularity of the trailing edge serration, in addition to the conventional trailing edge, a total of 12 different blades with serrated trailing edges as shown in figure 11(a), were designed and tested in this experiment. Table 1 gives the design parameters for all the serrated trailing edge configurations, and figure 11(b) shows the definition of the sawtooth amplitude ( $2h$ ) and the sawtooth wavelength ( $w$ ). In table 1, the  $c$  is the chord of the blade.



(a) the blade with serrated trailing-edge (b) The serrated TE parameter definitions  
Figure 10. The serrated trailing-edge blade and parameter definitions

Table 1 Design parameters of the trailing edge serrated configuration

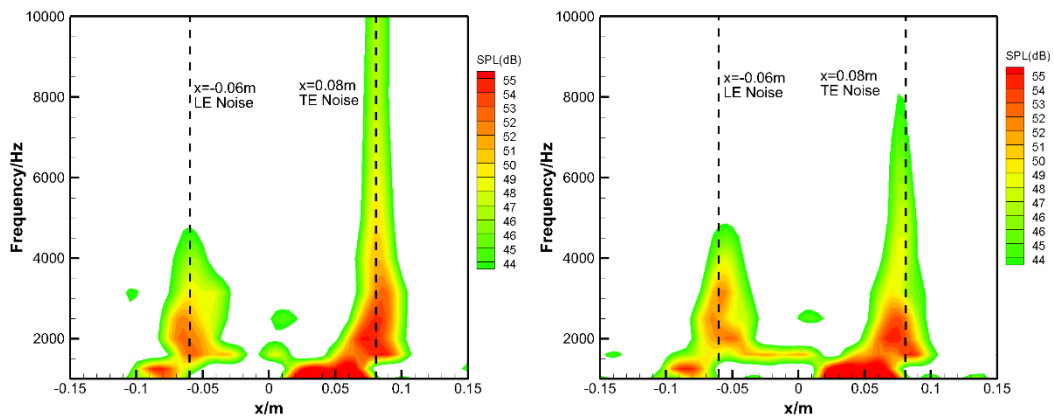
序号	名称	$2h$ (mm)	$2h/\bar{c}$	$\lambda$ (mm)	$\lambda/\bar{c}$	$\lambda/h$
0	Baseline	0	0	-	-	-
1	H5 $\lambda$ 3	5	0.033	3	0.02	1.2

2	H10 $\lambda$ 3	10	0.067	3	0.02	0.6
3	H15 $\lambda$ 3	15	0.100	3	0.02	0.4
4	H20 $\lambda$ 3	20	0.133	3	0.02	0.3
5	H25 $\lambda$ 3	25	0.167	3	0.02	0.24
6	H30 $\lambda$ 3	30	0.200	3	0.02	0.20
7	H40 $\lambda$ 3	40	0.267	3	0.02	0.15
8	H30 $\lambda$ 1.5	30	0.200	1.5	0.01	0.10
9	H30 $\lambda$ 5	30	0.200	5	0.03	0.33
10	H30 $\lambda$ 10	30	0.200	10	0.07	0.67
11	H30 $\lambda$ 15	30	0.200	15	0.10	1.00
12	H30 $\lambda$ 30	30	0.200	30	0.20	2.00

## 4.2 Experimental Results and Analysis

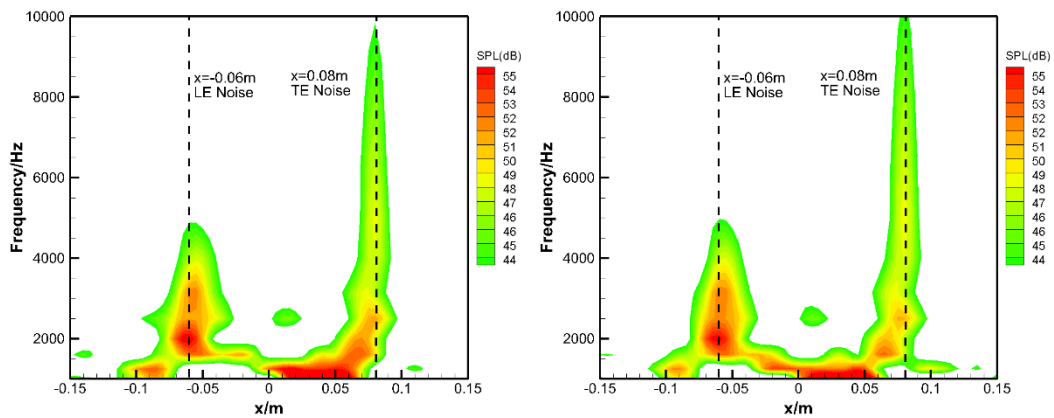
### 4.2.1 Effect of sawtooth amplitude on the trailing-edge noise reduction

Firstly, the influence of the amplitude of the trailing edge sawtooth on the trailing edge noise characteristics is investigated. Figure 11 shows the sound source identification maps of different amplitudes of trailing edge serrations under the conditions of flow velocity 40m/s and with sawtooth wavelength  $\lambda=3$ mm. It can be seen from the figure that TE noise can be significantly reduced with the serrated trailing-edge. It can also be seen from the figure 11(b) that the sawtooth trailing-edge has obvious noise reduction effect for high-frequency noise.



(a) Baseline

(b) H5 $\lambda$ 3



(c) H10 $\lambda$ 3

(d) H15 $\lambda$ 3

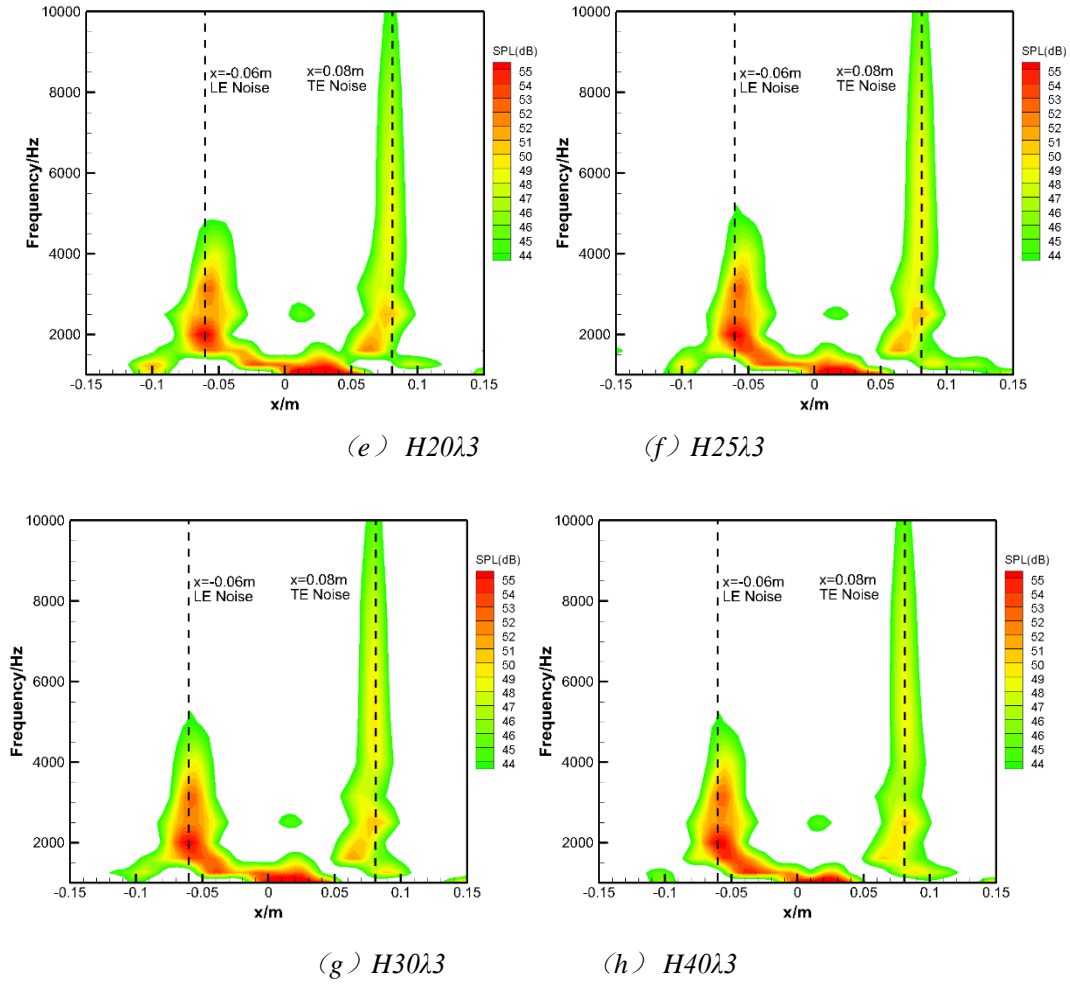


Figure 11 The sound source distribution of the blade with different sawtooth amplitudes (40m/s, angle of attack is 0 degree)

It could be seen from the beamforming results that the main lobe of LE and TE all have some width in space. The magnitude of the LE and TE noise should be the sum of sound level in specified space. In this study, the sound pressure level of LE and TE noise are calculated by the following equation,

$$L_{LE} = 10 \cdot \lg \left( \frac{\sum_{n=N_{min}}^{N_{max}} 10^{0.1L_n}}{N_{max} - N_{min} + 1} \right) \quad (7)$$

$L_n$  is the sound pressure level at position  $n$ . Suppose that the LE and TE noise source center is at the position of maximum sound pressure level (OASPL in frequency range of 1000Hz to 10000Hz),  $N_{min}$  is the upstream position where the OASPL is smaller of 3 dB than the maximum OASPL, and  $N_{max}$  is the downstream position where the OASPL is smaller of 3 dB than the maximum OASPL.

Figure 12 shows a 1/3 octave spectrum of the trailing edge noise for the blade with different sawtooth amplitudes and with the sawtooth wavelength of 3mm at airflow speed of 20m/s, 40m/s, 60m/s and 70m/s. It can be seen from Figure 12 that the trailing edge serrations can effectively reduce the TE noise. At the flow speed of 20 m/s and in the frequency range below 8000Hz, the noise can be reduced by 4-5 dB. When the airflow velocity is of 40 m/s, except  $H5\lambda_3$  serration configuration, the noise reduction effect of other serrated trailing-edge configurations is not significantly different, which can significantly reduce the blade TE noise at frequencies below 5000 Hz. However, when the frequency is above 5000Hz, the noise reduction effect is obviously weakened. With the increase of airflow velocity and when the airflow speed reaches 60 m/s and 70 m/s, the noise reduction difference between different sawtooth configurations increases. With the increase of the amplitude of serrations, the noise reduction increases.

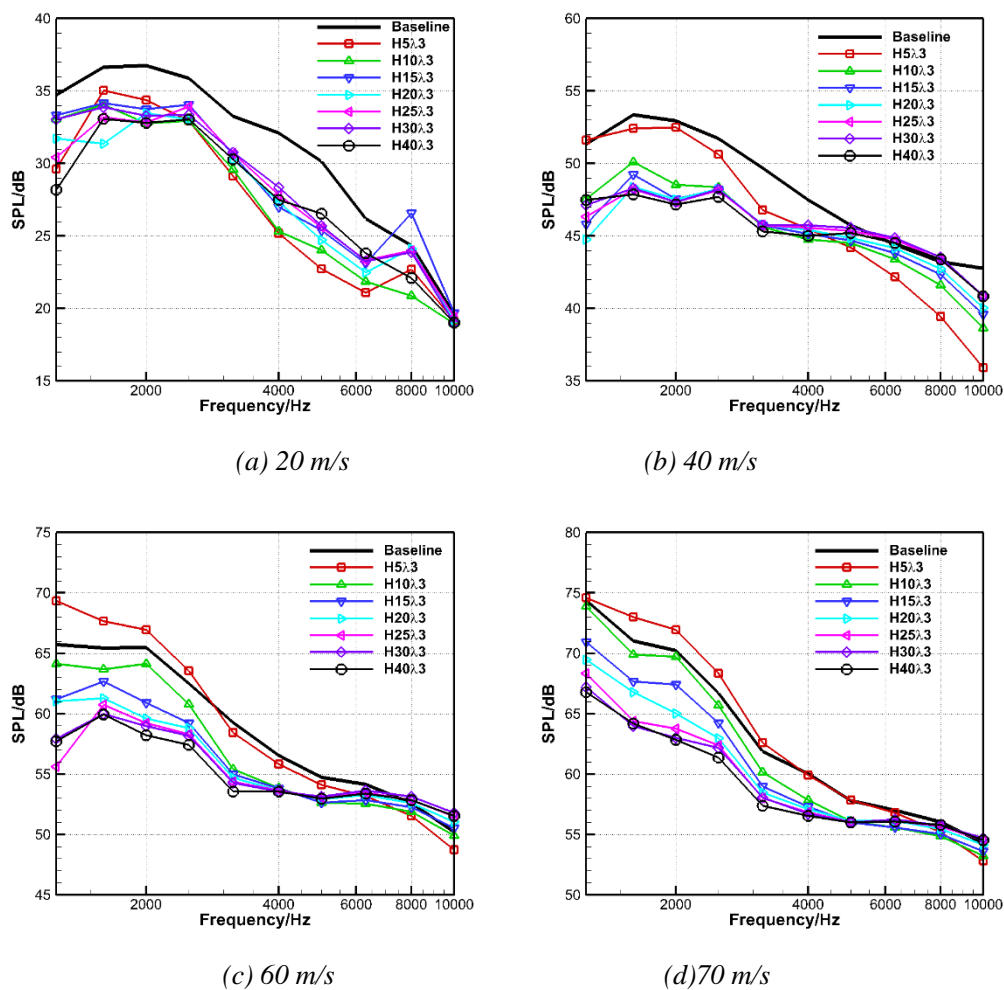


Fig12 Spectrum of the trailing edge noise with different sawtooth amplitudes( $\lambda=3\text{mm}$ )

#### 4.2.2 Effect of sawtooth wavelength on the trailing-edge noise reduction

Figure 13 shows a 1/3 octave spectrum of the trailing edge noise for the blade with different sawtooth wavelength and with the sawtooth amplitudes of 30mm at airflow speed of 20m/s, 40m/s, 60m/s and 70m/s. It can be seen from Figure 13 that, at the flow speed of 20 m/s, the  $H30\lambda_{1.5}$  sawtooth configuration has the large noise reduction, in the frequency range

of 1250Hz-10000Hz, the noise can be reduced by 3-4 dB. When the airflow velocity is of 40 m/s, the trailing edge serrations can effectively reduce the TE noise at the frequency below 4000Hz. However, when the frequency is above 4000Hz, the noise reduction effect is obviously weakened, and in some frequency, the TE noise will be enlarged. With the increase of airflow velocity and when the airflow speed reaches 60 m/s and 70 m/s, the noise reduction difference between different sawtooth configurations increases. The serrations with the smallest wavelength  $H30\lambda 1.5$  have the smallest noise reduction, and the serrations  $H30\lambda 10$  have the largest noise reduction.

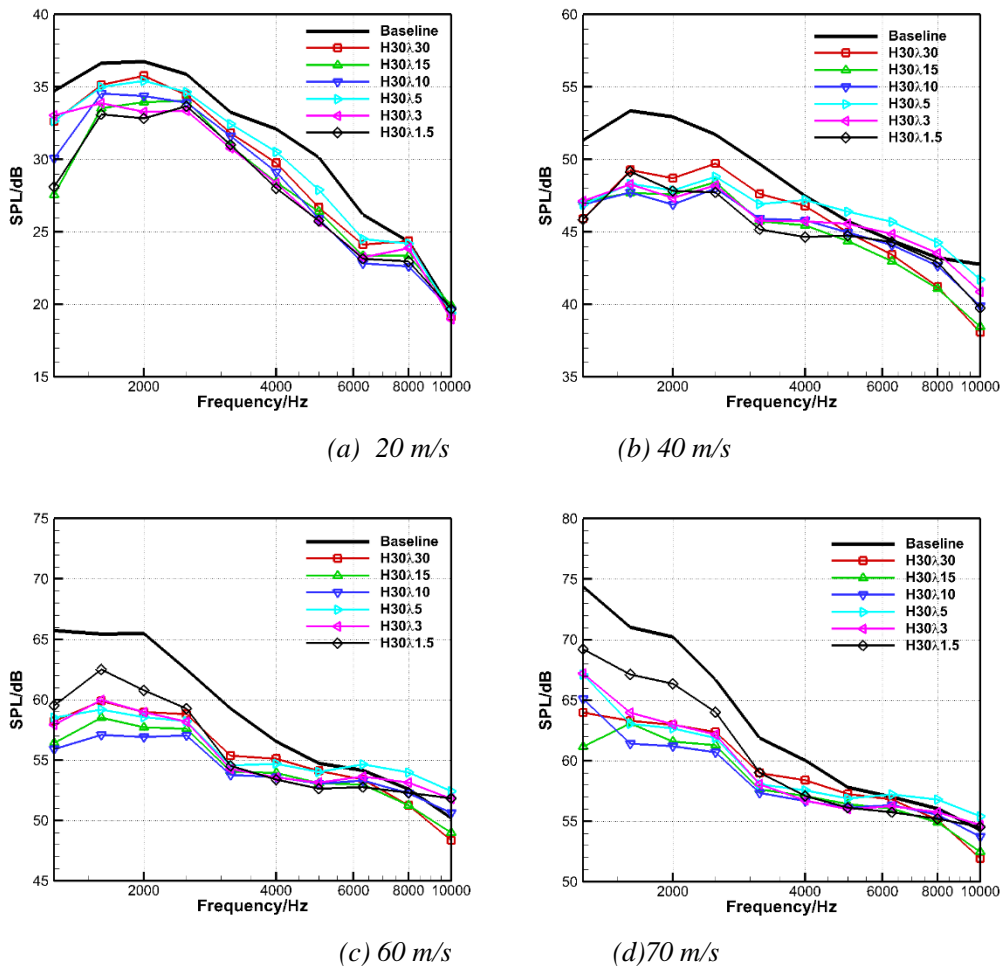


Fig13 Spectrum of the trailing edge noise with different sawtooth wavelength( $H=30\text{mm}$ )

## 5 CONCLUSIONS

The source identification technology based on the Clean-SC algorithm with microphone array was successfully used in this study to investigate the NACA65 (12)-10 blade TE noise reduction using serrated trailing-edge configuration in an indoor open jet wind tunnel test bed. Clear and quantitative sound radiation results from the NACA65 (12)-10 blade TE noise source are obtained. According to this study, some conclusions can be drawn below.

(1) The present array data reduction program which is based on Clean-SC algorithm was assessed using Sarradj's benchmark synthesized input data. As indicated by Sarradj, although Clean-SC algorithm has been proposed for a long time, it still needs special attention to its

correct application to achieve the best effect. The assessment results show that the present array data processing software based on Clean-SC algorithm has a good accuracy with an error of less than 0.5 dB in a wide frequency range.

(2) In the present blade leading-edge and trailing-edge noise tests, it is found that the noise level of the sound source identified by Clean-PSF algorithm is about 2dB higher than that identified by Clean-SC algorithm. This result shows that it is necessary to consider the influence of the interference of the sound sources on the identification using microphone array.

(3) The blade TE noise could be effectively reduced using serrated trailing edge. However, it should be noted that the amplitude and wavelength of the serrations will significantly affect the noise reduction. The flow speed and the angle of attack will also affect the noise reduction of serrated trailing-edge. In order to obtain the large noise reduction, the sawtooth configuration should be carefully designed according to the actual working conditions and air flow parameters.

## ACKNOWLEDGEMENT

The present work is supported by the National Natural Science Foundation of China (Project Grant No. 51936010 and No. 51776174 ), and Supported by National Science and Technology Major Project (2017-II-0008-0022).

## REFERENCES

1. Glibe, P.R., "Observations on Fan Rotor Broadband Noise Characteristics," 10th AIAA/CEAS Aeroacoustics Conference Proceedings, No. 2004-2909, AIAA, Manchester, England, 2004.
2. Curle, N., 1955. The influence of solid boundaries upon aerodynamic sound. Proc. Roy. Soc. (London) A321, 505-514.
3. Ffowcs Williams, J.E. and Hall, L.H., 1970. Aerodynamic sound generation by turbulent flow in the vicinity of a scattering half plane. J. Fluid Mech., 40, 657-670.
4. Crighton, D.G. and Leppington, F.G., 1970. Scattering of aerodynamic noise by a semi-infinite compliant plate. J. Fluid Mechanics, 43, 721-736
5. Crighton, D.G., 1972. Radiation from vortex filament motion near a half plane. J. Fluid Mechanics, 51, 2, 357-362
6. Chandiramani, K.L., 1974. Diffraction of evanescent waves, with application to aerodynamically scattered sound and radiation from un baffled plates. J. of the Acoustic Society of America, 55, 1, 19-29
7. Levine, H., 1975. Acoustical diffraction radiation. Philips Research Report, 30, 240-276
8. Howe, M.S., 1975. The generation of sound by aerodynamic sources in an inhomogeneous steady flow. J. Fluid Mechanics, 67, 3, 597-610
9. Howe, M.S., 1976. The influence of vortex shedding on the generation of sound by convected turbulence. J. Fluid Mechanics, 76, 4, 710-740
10. Chase, D.M., 1972. Sound radiated by turbulent flow off a rigid half-plane as obtained from a wavevector spectrum of hydrodynamic pressure. J. of the Acoustic Society of America, 52, 3, 1011-1023
11. Chase, D.M., 1975. Noise radiated from an edge in turbulent flow. AIAA J., 13, 8, 1041-1047
12. Davis, S.S., 1975. Theory of discrete vortex noise. AIAA J., 13, 3, 375-380
13. Howe, M.S., 1978. A review of the theory of trailing edge noise. J. Sound and Vibration, 61, 3, 437-465
14. Marcolini M., Brooks T., and Pope D., "Airfoil self-noise and prediction," NASA RP-1218, 1989.
15. Brooks T., and Hodgson T., "Trailing edge noise prediction from measured surface pressures," Journal of Sound and Vibration, Vol. 78, No. 2, 1981, pp. 69-117.
16. Amiet R., "Noise due to turbulent flow past a trailing edge," Journal of Sound and Vibration, Vol. 47, No. 3, 1976, pp. 387-393.
17. Amiet R., "A note on edge noise theories," Journal of Sound and Vibration, Vol. 78, No. 4, 1981, pp. 485-488.
18. Howe M. S., "Trailing edge noise at low mach numbers," Journal of Sound and Vibration, Vol. 225, No. 2, 1999, pp. 211-238.

19. Adams H., Patent Application for a “Noiseless device,” No. US2071012A, filed 22 Feb. 1937.
20. Graham R., “The silent flight of owls,” Roy. Aero. Soc. J, Vol. 286, 1934, pp.837-843.
21. Lilley G. M., “A study of the silent flight of the owl,” 4th AIAA/CEAS Aeroacoustics Conference, No.1998-2340, AIAA, Toulouse, France, 1998.
22. Bohn A., “Edge noise attenuation by porous edge extensions,” 14th AIAA Aerospace Sciences Meeting, No. 76-80, Washington, DC, 1976.
23. Khorrami M. and Choudhari M., “Application of passive porous treatment to slat trailing edge noise,” NASA TM-212416, 2003.
24. Sarradj E. and Geyer T., “Noise generation by porous airfoils,” 13th AIAA/CEAS Aeroacoustics Conference, No. 2007-3719, Rome, Italy, 2007.
25. Finez A., Jondeau E., Roger M., and Jacob M., “Broadband noise reduction with trailing-edge brushes,” 16th AIAA/CEAS Aeroacoustics Conference Proceedings, No. 2010-3980, Stockholm, Sweden, 2010.
26. Howe M. S., “Aerodynamic noise of a serrated trailing edge,” Journal of Fluid and Structures, Vol.5, No.1, 1991, PP.3-45.
27. Howe M. S., “Noise produced by a sawtooth trailing edge,” J. Acoust. Soc. Am., Vol. 90, No. 1, 1991, pp.482-487.
28. Oerlemans S., Fisher M., Maeder T., and Kogler K., “Reduction of wind turbine noise using optimized airfoils and trailing-edge serrations,” NLR-TP-2009-401, 2009.
29. Gruber, M., Joseph, P. F. and Chong, T. P., “Experimental Investigation of Airfoil Self Noise and Turbulent Wake Reduction by the Use of Trailing Edge Serrations,” 16th AIAA/CEAS Aeroacoustic Conference, No.2010-3803, Stockholm, Sweden, 2010.
30. Ji Liang, Experimental and numerical study on mechanism and suppression method of turbo-machinery broadband noise[D]. Ph.D thesis, Northwestern Polytechnical University. 2016.
31. Michel U., “History of acoustic beamforming,” Berlin Beamforming Conference(BeBeC), 21-22, Nov. 2006.
32. Venkatesh S.R., Polak D.R., and Narayanan S., “Beamforming algorithm for distributed source localization and its application to jet noise”, AIAA Journal, Vol. 41, NO. 7, 2003, pp. 1238-1246.
33. Lowis C., and Joseph P., “A focused beamformer technique for separating rotor and stator-based broadband sources”, 12th AIAA/CEAS Aeroacoustics Conference, No. 2006-2710, 2006.
34. Brooks, T. F., Humphreys, W. M., “A deconvolution approach for the mapping of acoustic sources (DAMAS) determined from phased microphone arrays,” Journal of Sound and Vibration, Vol. 294, 2006, pp. 856-879.
35. Brooks, T. F., Humphreys, W. M., Plassman, G. E., “DAMAS processing for a phased array study in the NASA Langley jet noise laboratory,” 16th AIAA/CEAS Aeroacoustics Conference, No. 2010-3780, 2010.
36. Sijtsma, P., “CLEAN based on spatial source coherence,” International journal of aeroacoustics, Vol, 6, 2007, pp. 357-374.
37. Sarradj, E., Herold, G., Sijtsma, P., et al., A microphone array method benchmarking exercise using synthesized input data[C]. 23rd Aiaa/ceas Aeroacoustics Conference, Aiaa Aviation Forum. 2017, AIAA 2017-3719.
38. Weiyang Qiao, Liang Ji, Fan Tong, Liangfeng Wang and Weijie Chen, Separation and Quantification of Airfoil Le- and Te-Noise Source with Microphone Array , 2018 Berlin Beamforming Conference, BeBeC2018 D-14, March 5-8, Berlin, Germany